

COMBINING POWER-LAW AND SURFACE-DRAG FLOW MODELS: A NEW APPROACH FOR IMPROVING ZONAL MODELS

Teshome E. Jiru and Fariborz Haghghat

Department of Building, Civil and Environmental Engineering, Concordia University,
Montreal, Quebec, Canada

ABSTRACT

This paper presents the methodology for combining the power-law model (PLM) with the surface-drag flow model (SDM). The two types of combination explored were the direct and the indirect approaches. The direct combination of SDM and PLM has provided three different forms of zonal models: SD-PLM1, SD-PLM2, and SD-PLM3. The indirect combination gave the modified power-law model (MPLM). The predictions of the models were compared with each other and with experimental data for isothermal and non-isothermal cases. The MPLM has provided the best predictions of the recirculation in the standard zone.

INTRODUCTION

Zonal airflow models are intermediate models between the extremes of single/multi-zone and CFD. For single/multi-zone model a zone may represent a building or a section of a building such as a room. However, in the zonal approach, a room can be divided into a number of control volumes, using two or three-dimensional cells, which are usually larger than the cells normally used in CFD applications. The advantage of using the zonal approach is that the resulting systems of algebraic equations are smaller and much easier to solve than the difference approximations to the partial differential equations used in the CFD approach. The zonal models can therefore provide information on airflow and temperature distribution in a room faster than CFD, but with more accuracy and detail than single/multi-zone models.

In the zonal method, conservation equations are formulated for each cell. The mass and energy conservation equations for each cell can be given as:

$$\sum m_{i,j} + S_M = 0 \quad (1)$$

$$\sum q_{i,j} + S_q = 0 \quad (2)$$

Where $m_{i,j}$ is the mass flow rate from cell i to cell j ; S_M is the mass source; $q_{i,j}$ is the heat flow; S_q is the

heat source. For the zonal approach, a zone can be categorized as either a specific or a standard flow zone (Haghghat et al. 2001; Inard et al. 1996; Wurtz, 1995). The specific flow zones include jets, plumes, heaters and boundary layer zones. The standard flow zone represents the large part of the room, which is not directly affected by the presence of specific zones. Due to the distinct characteristics of the airflow in the standard and specific zones, different models have been used to describe the airflow in each zone. The airflow equations used in specific flow zones and standard flow zones are referred to as non-pressure and pressure flow models, respectively (Teshome and Haghghat, 2004). Megri et al. (2005) also classified the zonal models as first, second and third generation models, which are non-pressure, pressure, and integration of the two, respectively. The non-pressure (first generation) airflow models are the earlier zonal models that employ empirical and analytical relations to express the mass flow in specific flow zones such as plumes and boundary layers (Inard, 1988). In the zonal approach, the mass flow rate for horizontal jet cells can be given as (Rajaratnam, 1976):

$$m_x = 0.25m_o \left(\frac{x}{h_o} \right)^{1/2} \quad (3)$$

Where m_x is the mass flow rate for a cell in the jet zone; m_o is the inlet mass flow rate; x is the horizontal distance of jet cell from the inlet; h_o is the inlet height/width. The pressure (second generation) airflow models employ the power-law model (PLM) to compute the mass flow rate in standard cells:

$$m_{i,j} = KA\rho \left(\frac{2\Delta P_{i,j}}{\rho} \right)^{1/2} \quad (4)$$

Where K is the flow coefficient; A is area of cell; ρ is density of air; $\Delta P_{i,j}$ is the pressure difference between cell i and j . The zonal approach in use today (the third generation) integrates non-pressure and pressure zonal airflow models to describe the flow field in a room. These models have been integrated with other models such as moisture transfer models (Mendoca et al. 2002), thermal comfort models (Haghghat et al. 2001), and contaminant source and

sink models (Huang et al. 2002); and COMIS (Ren and Stewart, 2003).

Accurate prediction of the flow field is a vital step since the prediction of the other scalars such as moisture, temperature and contaminant distribution highly depends on it. In the zonal approach, the prediction of the velocities in specific zones is reasonably accurate since well-developed empirical relations, such as Equation 3, are used. However, the PLM, which is used in the standard zones, has been able to predict the flow field reasonably well only for natural convection (Haghighat et al. 2001). For the case of forced convection, the PLM has shown pronounced discrepancies in predicting the recirculation in the standard zone (Haghighat et al. 2001; Mora et al. 2003).

The PLM is a one-dimensional model - no flow information is included from the other direction. As can be seen in Equation 4, the mass flow rate is calculated from the pressure difference in the flow direction. The PLM is similar to the power-law equation used for flow through cracks and orifices. In the case of flow through cracks and orifices, the values of the pressure difference $\Delta P_{i,j}$ is obtained from pressures measured at points away from the opening so that the influence of the flow is negligible. The orifice equation is therefore a reasonable model when the kinetic energy of the air flowing through small openings and cracks is completely dissipated in the static room air (Kato, 2004). Nevertheless, this hydrostatic field assumption, which is used for the definition of the discharge coefficient (Sandberg, 2004; Etheridge, 2004) has also been applied in the implementation of the PLM to relate the pressures in each cell in the standard zone. Hence, the roots of the discrepancies of the zonal model can be traced back to such assumptions used in applying the PLM to describe the airflow in the standard zone.

The standard zone is the low velocity zone and is considered to be unaffected by the flow in specific zones. Indeed, original developers of the zonal model were aware of this problem but few efforts were made to improve the PLM for indoor airflow application. Axley (2001) has attempted to improve the PLM using an alternative approach: the surface-drag flow model (SDM). He used the momentum balance near wall surfaces, and the mixing length and eddy viscosity expression for turbulent flow. He assumed a well-developed duct flow velocity profile along the direction perpendicular to the nearest wall. Moreover, a parameter was used to tune the SDM for cells far from the wall. Nevertheless, comparisons of the flow field predicted by the PLM and the SDM showed that the SDM with its existing form has made no significant improvement in predicting the

recirculation (Mora et al. 2003). Furthermore, Teshome and Haghighat (2005) have employed another approach: use of different flow coefficient (K) for each cell. They obtained improvement in the prediction of the recirculation in the standard zone but the limitation of their approach was that it cannot be generalized for other room configuration. In this regard, this paper presents a new methodology for the improvement of the PLM by combining the PLM with the SDM.

COMBINING THE PLM AND THE SDM

The difficulty of generalizing the PLM with variable flow coefficient (Teshome and Haghighat, 2005) coupled with the discrepancies of SDM and PLM predictions have led the pursuit of the proposed methodology for the improvement of PLM - combining PLM and SDM. Two approaches were employed: direct and indirect. In the direct approach the $\Delta P_{i,j}$ and $m_{i,j}$ in SDM and PLM were added to get the total pressure drop and mass flow rate between two cells, while in case of the indirect approach analogies of flow between parallel plates were used to modify and combine the SDM with the PLM.

The direct approach

The first direct approach for the combination of the PLM and the SDM leads to the following general relation for zonal models:

$$\Delta p_{i,j} = am_{i,j}^2 + bm_{i,j} \quad (5)$$

Where the coefficients a and b are a function of the type of zonal model as given in Table 1.

The second direct combination gives the combined SDM and PLM type 3 (SD-PLM3):

$$m_{i,j} = a\Delta p_{i,j}^{0.5} + b\Delta p_{i,j} \quad (6)$$

Where the coefficients a and b for Equation 6 are also given in Table 1. Similar equations with different coefficients were also developed for crack flow (Chiu and Etheridge, 2002). The similarity is not a coincidence given the fact that the power-law in Equation 4 commonly used in the zonal models was originally used for flow through cracks and large openings. Moreover, the linear and the nonlinear terms in Equation 6 have been commonly used independently in the implementation of PLM (Haghighat et al. 2001). The linear term is invoked at smaller pressure differences whereas the non-linear is invoked at higher ones.

Simulations were conducted to compare the prediction capability of the combined models in the standard zone. An isothermal room with two-dimensional slot diffuser was selected. The inlet and outlet are on the same wall; the inlet close to the ceiling and the outlet close to the floor. The inlet velocity (U_0) = 3.47m/s, room length (L) = 5.4m,

room height (H) = 2.5m, inlet height = 0.01m, and outlet height = 0.125m (Nielsen, 1998). The velocity measurements in the room were made with a low velocity flow analyzer type 54N10 from Dantec with accuracy of about 0.04m/s (Nielsen, 1998). Equation 3 was applied to describe the airflow rate for cells in the jet zone. The room was divided into 11x11 cells. Since values of K other than 0.83 have made no difference in the prediction of PLM, the value of K for all combined models with $a \neq 0$ was set to 1.0 for all cells in the standard zone. Furthermore, the SDM1 and SD-PLM2 were not included in the comparison. This is because the linear SDM1 is similar to the power-law for smaller pressure differences. Moreover, Axley (2001) has suggested that the linear SDM1 can only serve as a preliminary solution to be used as initial guess for the nonlinear SDM2. The combined SD-PLM2 is simply the PLM with value of K other than 1.0, which was found to have no impact on the prediction.

Figure 1 depicts the comparison of the measured and the predicted dimensionless horizontal velocity (U/U_0) profile by the PLM, SDM2, SD-PLM1, and SD-PLM3 at vertical position 3m from the inlet. In Figure 1, the predictions of all the models do not show any tendency to follow the measured profile. For all models the magnitudes of the predicted velocities have discrepancies compared to measured values except at the inlet position ($y/H > 0.8$) due to the use of Equation 3. All the models predicted low velocity in the standard zone. These comparisons show that direct approach of combining the PLM and the SDM cannot predict recirculation in the standard zone.

The indirect approach

The physical basis for the indirect approach for combining the PLM and the SDM can be initiated by observing closely the discrepancies pertaining to these models. In the PLM approach, information of the flow is transmitted from cell to cell only through the pressure in the flow direction. This has produced back flow in all cells in the standard zone when the pressure gradient in the flow direction is negative. In the zonal approach, the cells in the standard zone are considered to have a low velocity and unaffected by the flow in the jet zone. The influence of the jet is therefore not accommodated outside the jet zone. To further clarify this, analogy with the combined Couette-Poiseuille flow between plates in Figure 2 can be considered. The Couette-Poiseuille flow can be given as:

$$\frac{u}{U_0} = 0.5 \left(1 + \frac{y}{H} \right) + C \left(1 - \frac{y^2}{H^2} \right) \quad (7)$$

Where the coefficient C is given by

$$C = \left(- \frac{\Delta P_x}{\Delta x} \right) \frac{H^2}{2\mu U_0} \quad (8)$$

Where u is the horizontal velocity at a distance y/H from bottom plate; U_0 is the maximum velocity; H is the gap height; μ is the air viscosity. Figure 2 shows that there is always a reverse flow in some part of the gap between the two plates when $C < 0.25$ (White, 1990). In those parts of the gap the negative pressure difference can be dominant and makes the contribution of the first term in the right hand side of Equation 7 negligible. A similar situation occurs in all cells in the standard zone since the PLM does not take into account the influence of the driving jet in those cells. Therefore, the PLM prediction in the standard zone can be considered as similar to the extreme case of the Couette-Poiseuille, or simply Poiseuille flow. Axley (2001) used the latter with some modifications for the derivation of the SDM. But, it was stated earlier that SDM has not improved the prediction compared to PLM.

Therefore, from the above discussion one can infer that in order to enhance the prediction capability of the PLM; the velocity in the dominant flow direction should not only depend on the pressure difference but also the magnitude of the maximum velocity at a vertical position. To that effect, one can insert Equations 7 and 8 into Equation 4 to derive the modified power-law model (MPLM):

$$u = K \left(\frac{\Delta P_x}{\rho} \right)^{n_1} + u_x \left(\frac{y}{H} \right)^{n_2} \quad (9)$$

$$v = K \left(\frac{\Delta P_y}{\rho} \right)^{0.5} \quad (10)$$

$$w = K \left(\frac{\Delta P_z}{\rho} \right)^{0.5} \quad (11)$$

Where n_1 is the power-law exponent; n_2 is the surface-drag exponent; u_x is velocity of the inlet air jet at a distance x from the inlet. The MPLM is therefore a modified form of the Couette-Poiseuille equation. In the former the room is considered as number of connected parallel plates (ceiling and floor); each like in Figure 2. However, unlike the Couette-Poiseuille, in the MPLM the pressure gradients in the directions normal to the dominant flow are not zero and the pressure gradient in the dominant flow direction is not known a priori; it is rather part of the solution. The introduction of the second term in Equation 9 makes sure that the influence of the driving air jet is taken into account for the cells in the standard zone. The influence of the jet is only included in the dominant jet flow direction, which is x for horizontal inlet velocity and y for vertical inlet velocity. This makes the second

term in Equation 9 to be known for all cells at the start of the solution for a given inlet condition.

Furthermore, two possibilities were explored for the value of u_x for each 'parallel plate' in a room. The first calculates u_x applying the air jet formula in Equation 3. The second uses a constant value of $u_x = U_0$. Simulation was then conducted for isothermal room with two-dimensional slot used in the direct approach (Nielsen, 1998). n_1 and n_2 in Equation 9 were given values of 1.0 and 2.0, respectively (the influence of n_1 and n_2 on the prediction is discussed in the next section). The recirculation for the first case is confined mostly close to the inlet side, while it covers the entire room for $u_x = U_0$ (Figure 3). The prediction for $u_x = U_0$ for all cells in the specific zone is more acceptable. Thus, in the following sections the predictions of the MPLM with $u_x = U_0$ will be compared with experimental data for isothermal and non-isothermal rooms.

RESULTS AND DISCUSSION

Isothermal room: wall inlet

The same room with a two-dimensional slot used in the direct approach for an inlet velocity of $U_0 = 3.47\text{m/s}$, (Nielsen 1998) was employed for the simulation. The simulations of the MPLM were conducted by varying first n_2 and then n_1 .

- Five values of were chosen for n_2 : 1/7, 0.5, 1.0, 1.5, and 2.0. $n_2 = 2.0$ and $n_2 = 1/7$ are used for laminar and turbulent velocity profiles for internal flow. The power-law exponent $n_1 = 0.5$ and $K = 1.0$ was used for all simulations of the MPLM (Equations 9 to 11). The comparisons of the velocity profile predicted by the MPLM for the five n_2 values at vertical position $x = 3\text{m}$ from the inlet side is depicted in Figure 4. The maximum predicted velocities close to the floor are smaller than the measured one. The differences can be attributed to the recirculation present in the room. It can also be observed from Figure 4 that increasing n_2 increases the magnitude of the velocity, except close to the floor. Comparing the air flow patten predicted for $n_2 = 1/7$ (not shown) with $n_2 = 2.0$ (Figure 3) shows that the former is more accurate for cells close to the floor whereas $n_2 = 2.0$ is more acceptable for cells at the center and close to the jet zone. But globally, the airflow pattern predicted when $n_2 = 2.0$ can be used with reasonable prediction of the magnitude of the velocity and the recirculation in the standard zone.
- To investigate the effect of the power law exponent, n_1 on the prediction of the MPLM. Two values for n_1 : 0.5 and 1.0 were used. The

values of $n_2 = 1$ and $n_2 = 2$ for $n_1 = 0.5$ from above were also chosen. This gives four combinations of n_1 and n_2 : ($n_1 = 0.5, n_2 = 1$); ($n_1 = 0.5, n_2 = 2$); ($n_1 = 1, n_2 = 1$); and ($n_1 = 1, n_2 = 2$). Simulations of the MPLM for the four combinations of n_1 and n_2 were then done. The result showed that changing n_1 from 0.5 to 1.0 has no significant influence on the magnitude of the predicted velocity.

Isothermal room:Ceiling inlet

For the ceiling inlet another room used for experimental and numerical study of room airflow by Nielsen (1998) was selected. The dimension of the room are $H = 2.8\text{m}$, $W = 4.0\text{m}$, and $L = 6.0\text{m}$. The inlet is a 0.02m wide three-dimensional slot across the width of the room. Four exhausts with dimension of 1.2x0.16m are positioned symmetrically on the ceiling. The air is discharged into the room in two opposite horizontal direction at an average inlet velocity $U_0 = 2.53\text{m/s}$. The velocity measurements in the room were also made with a low velocity flow analyzer type 54N50 from Dantec with accuracy of about 0.04m/s. Simulation of the MPLM was conducted for two cases: 15x3x5 cells and 15x3x10 cells. Due to the aforementioned reason, $n_1 = 1$ and $n_2 = 2$ was used. $K = 1.0$ was also used as it was also found that other values of K did not change the prediction quality. The airflow fields predicted by the MPLM for 15x3x10 cells is depicted in Figure 5. The MPLM predicted the recirculation region at both sides of the inlet. Figure 6 illustrates the comparison of prediction of the MPLM and measured values at $x = 1\text{m}$ from the left wall. It can be seen that the prediction follows the measured velocity profile for both 15x3x5 and 15x3x10 cells. Close to the floor the measured velocities are higher. But, the predicted velocities are within the range of accuracy of the measurement. Moreover, increasing the number of cells has increased the accuracy of the prediction below the center of recirculation.

Non-isothermal room

A non-isothermal room, shown in with $L = 5.5\text{m}$, $W = 3.7\text{m}$, and $H = 2.4\text{m}$, $h_o = 0.05\text{m}$, and outlet width = 0.2m (Zhang et al. 1992; Zhao, 2000) was selected. The average inlet air velocity (U_0) = 1.78 m/s. The heating capacity (178W/m^2) can raise the average room air temperature (T_{indoor}) to 32°C. The test room and the exhaust plenum chamber were well insulated so that the heat loss through the walls, ceiling, and floor can be neglected (Zhang et al., 1992). Zhang et al. (1992) and Zhao (2000) measured the air temperature and air velocity distribution in this room: Zhang et al. (1992) used the hot wire technique and Zhao (2000) used the PIV (Particle Image Velocimetry) technique.

The major forces exerted on the air jet in the non-isothermal condition are inertia and thermal buoyancy. Therefore, for the non-isothermal an important parameter. It limits the penetration length (L_p) of the air jet. The critical Ar_0 is a limiting value above which the diffuser air jet drops immediately after entering the room. For $T_0 = 24\text{ }^\circ\text{C}$, $T_{indoor} = 32\text{ }^\circ\text{C}$, $U_0 = 1.78\text{ m/s}$ and $h_0 = 0.05\text{ m}$, $Ar_0 = 0.004056$. Since $Ar_0 < 0.023$, the air jet cannot immediately drop after entering the room and L_p is approximately equal to 3.3m (Figure 7). The MPLM was directly applied in the region $0 < x < L_p$. But the second term in Equation 9 was set to zero in the region $L_p < x < L$ due to the absence of the air jet in this region. Additionally, as per the description of the experimental set-up, all the surfaces except the floor are assumed adiabatic.

Figure 7 depicts the measured airflow pattern in the non-isothermal. Comparison of the MPLM predictions in Figure 8 with Figure 7, shows that the MPLM like the measured airflow pattern predicts one recirculation zone within with in the range $0 < x < L_p$. The measured airflow pattern also shows another smaller and weaker recirculation near the air outlet. But, the MPLM shows only the tendency to form this weaker recirculation. The comparison of the air velocity predicted by the MPLM and the PLM with measured data at $H = 1.7\text{ m}$ from the floor shows that the MPLM prediction is superior to that of the PLM. Furthermore, the measured and predicted air temperature distributions in the room are shown in Figures 9 and 10, respectively. As shown in Figures 7 and 8, the recirculation draws air from outlet side

condition, the Archimedes number (Ar_0), which is the ratio of thermal buoyancy force to inertia force is

to the inlet side. Since the floor further heats this warm air, the inlet side in Figures 9 and 10 is always warmer than the outlet side. Comparing Figure 10 with Figure 9, it can be seen that the MPLM predicts the temperature well close to the inlet and outlet. However, for the PLM it was found that the higher temperatures are close to the inlet and outlet region. This is because the air jet falls rapidly, after entering the room, drawing warm air to the inlet side; and the region outside of the recirculation region moves the warm air to the outlet side leaving the occupied region at a lower temperature than either side of the room. This clearly indicates one of the important reasons for predicting the recirculation region in the standard zone.

CONCLUSION

The methodology for combining PLM and SDM was presented using the direct and the indirect approaches. The models obtained using the direct approach: SDM1, SDM2, SD-PLM1, SD-PLM2, and SD-PLM3, were found to be unable to predict recirculation in the standard zone compared to experimental data. However, the MPLM, which is the result of the indirect approach, was found to predict the flow field reasonably well in standard zone for isothermal and non-isothermal rooms. The inclusion of the influence of the air jet in the MPLM for the dominant flow direction has made the MPLM to be superior to all the other zonal models in predicting the recirculation region.

FIGURES AND TABLES

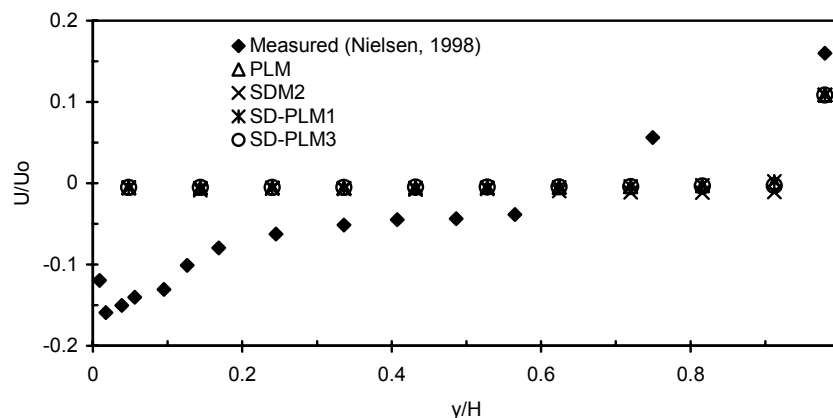


Figure 1 Comparison of the zonal models predictions with experimental at $x = 3\text{ m}$ for wall inlet.

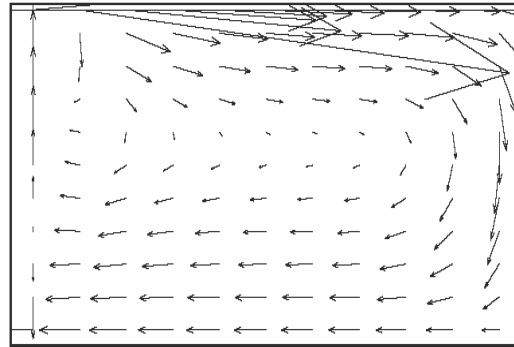
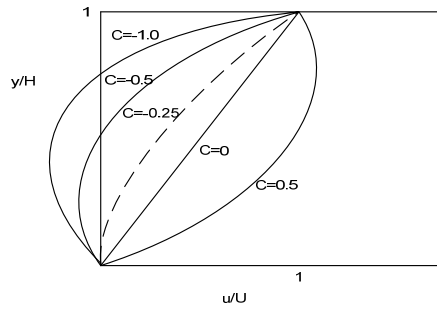


Figure 2 The Couette-Poiseuille flow (White, 1990). Figure 3 Airflow pattern predicted by the MPLM.

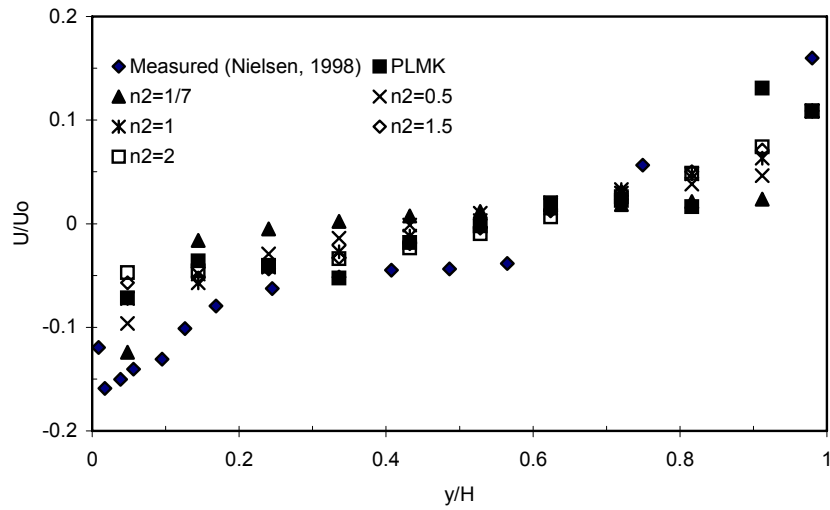


Figure 4 Comparison of the MPLM predictions for different values of n_1 and n_2 with measured data at $x = 3m$ for wall inlet.

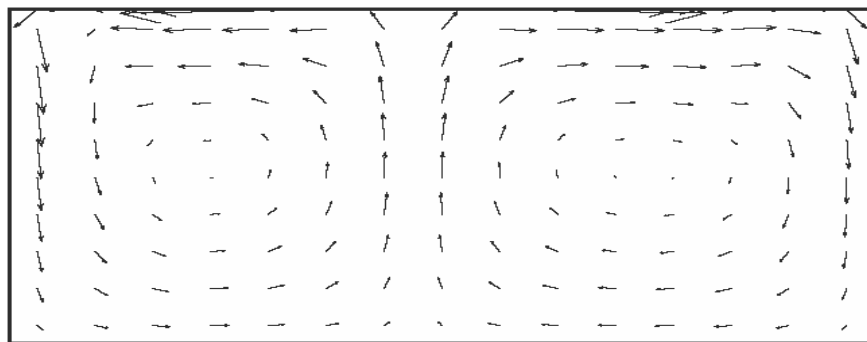


Figure 5 Airflow pattern predicted by the MPLM using 15x3x10 cells for ceiling inlet.

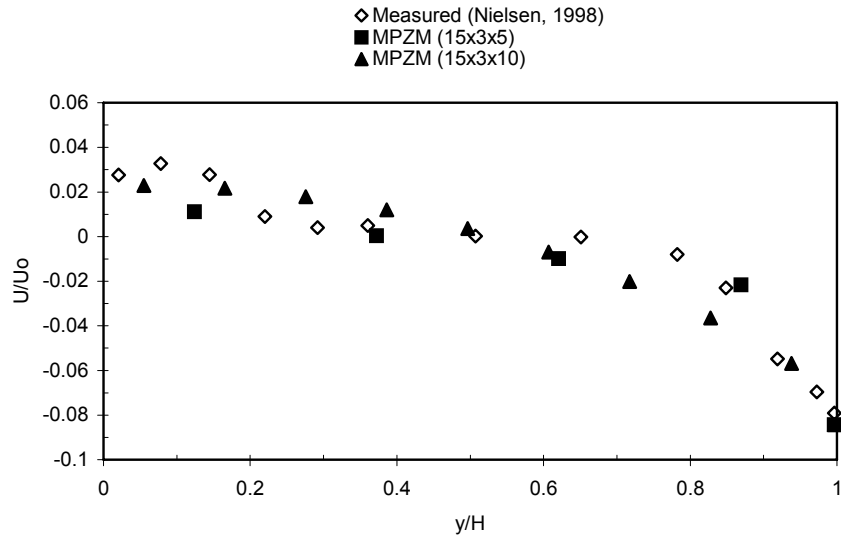


Figure 6 Comparison of the MPLM predictions with measured data at $x = 1.0\text{m}$ for ceiling inlet.

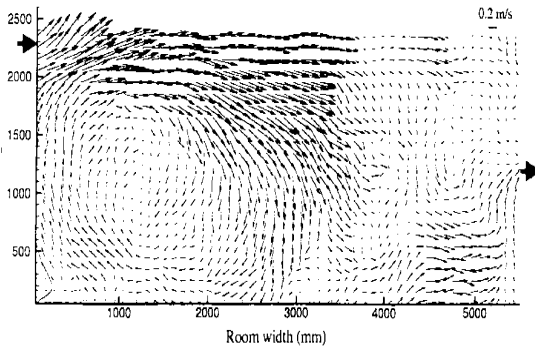


Figure 7 Measured airflow pattern (Zhao, 2000).

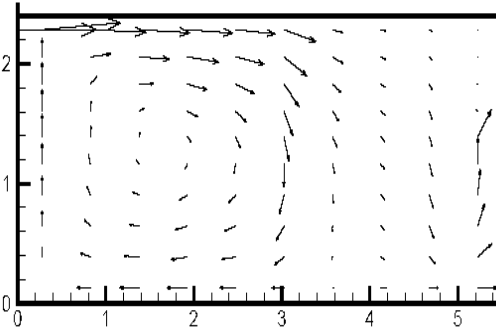


Figure 8 The MPLM airflow pattern prediction for non-isothermal room.

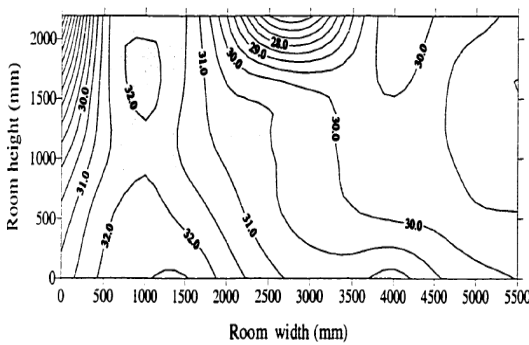


Figure 9 Measure temperature distribution (Zhao, 2000).

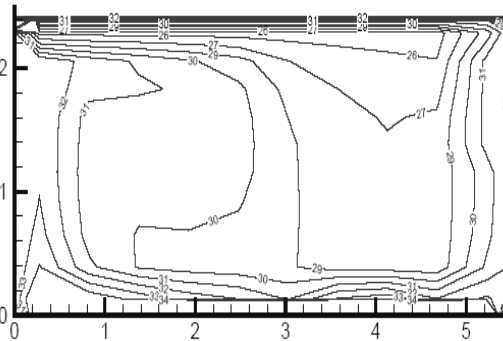


Figure 10 Temperature distribution predicted by the MPLM.

Table 1
Summary of zonal models

| Model | a | b |
|---------|--|---|
| PLM | $\frac{1}{2K^2 A^2 \rho}$ | 0 |
| SDM1 | 0 | $\frac{\mu_e \pi^2 \Delta x}{4 \rho Y^2 A}$ |
| SDM2 | $\frac{2k_s \kappa^2 a^3 \Delta x}{\rho A^2 \Delta y}$ | 0 |
| SD-PLM1 | $\frac{1}{2K^2 A^2 \rho}$ | $\frac{\mu_e \pi^2 \Delta x}{4 \rho Y^2 A}$ |
| SD-PLM2 | $\frac{2k_s \kappa^2 a^3 \Delta x}{\rho A^2 \Delta y} + \frac{1}{2K^2 A^2 \rho}$ | 0 |
| SD-PLM3 | $KA\sqrt{2\rho}$ | $\frac{4\rho Y^2 A}{\mu_e \pi^2 \Delta x}$ |

REFERENCES

- Axley JW. 2001. Surface-drag flow relations for zonal modeling, *Building and Environment*, 36, pp843-850.
- Chiu and Etheridge, D.W. 2002. Calculation and notes on the quadratic and power-law equations for modeling infiltration, *International journal of ventilation*, 1(1), pp65 -77.
- Etheridge, D.W. 2004. Natural ventilation through large openings – measurements at model scale and envelope flow theory. *International journal of ventilation*, 2(4), pp 325 – 342.
- Haghighat F, Li Y and Megri AC. 2001. Development and validation of a zonal model-POMA, *Building and Environment* 36, pp1039-1047.
- Huang, H, Haghighat F. and Wurtz E. 2002. An integrated zonal model for predicting transient VOC distribution in ventilated room. *Proceedings of Esim 2002*, Montreal, Canada, 78-83.
- Inard C. 1988. Contribution a l'étude du couplage thermique entre une source de chaleur et un local, *Ph.D Thesis*, INSA de Lyon, France.
- Inard C, Bouia H and Dalicieux P.1996. Prediction of air temperature distribution in buildings with a zonal model, *Energy and Buildings*, 24, pp125-132.
- Kato S. 2004. Flow network model based on power balance as applied to cross-ventilation,

- International journal of ventilation*, 2(4), pp395 – 408.
- Mendoca, K.C. Inard, C. Wurtz, E. and Winkelmann, F.C. 2002. A zonal model for predicting simultaneous heat and moisture transfer in buildings. *Indoor air* 2002.
- Megri A.C, Snyder M and Musy M. 2005. Building zonal thermal and airflow modeling – a review, *International journal of ventilation*, 4(2), pp177 – 188.
- Mora L, Gadgil J and Wurtz E. 2003. Comparing zonal and CFD model predictions of isothermal indoor airflows to experimental data, *Indoor air*, 13, pp77-85.
- Nielsen, J.R.1998. The influence of office furniture on the air movements in a mixing ventilation room, *Ph.D Thesis*, Aalborg University, Denmark.
- Rajaratnam N. 1976. *Turbulent Jets*. Elsevier Scientific Publications, New York, USA
- Ren, Z. and Stewart, J. 2003. Simulating airflow and temperature distribution inside buildings using a modified version of COMIS with sub-zonal divisions. *Energy and Buildings*, 35:257-271.
- Sandberg, M. 2004. An alternative view on the theory of cross-ventilation, *International journal of ventilation*, 2(4), pp 409 – 418.
- Teshome, E.J. and Haghighat, F. 2004. Zonal models for indoor airflow – a critical review, *International journal of ventilation*, 3(2), pp 119 - 129.
- Teshome, E.J. and Haghighat, F. 2005. Macroscopic and microscopic analysis of zonal model. The 9th IBPSA Conference, Montréal, Canada, August 15th to 18th 2005.
- White F.M. 1991. *Viscous fluid flow*, McGraw-Hill series in mechanical engineering, New York.
- Wurtz, E.1995. Modelisation tridimensionnelle des transferts thermiques et aerauliques dans le batiment en environnement oriente objet. *Ph.D. Thesis*, ENPC, France
- Zhang, J.S.1991. A fundamental study of two-dimensional room ventilation flows under isothermal and non-isothermal conditions. *PhD Thesis*, University of Illinois, Urbana USA.
- Zhao, L. 2000. Measurement and analysis of full-scale room airflow using particle image velocimetry (PIV) technique. *PhD Thesis*, University of Illinois, Urbana, USA